

## Reverse-phase h.p.l.c. separation, quantification and preparation of bilirubin and its conjugates from native bile

Quantitative analysis of the intact tetrapyrroles based on h.p.l.c. of their ethyl anthranilate azo derivatives

William SPIVAK\* and Martin C. CAREY†

Departments of Medicine and Pediatrics, Harvard Medical School, Divisions of Gastroenterology, Brigham and Women's Hospital, and Children's Hospital Medical Center, Boston, MA 02115

(Received 6 August 1984/Accepted 2 October 1984)

We describe a facile and sensitive reverse-phase h.p.l.c. method for analytical separation of biliary bile pigments and direct quantification of unconjugated bilirubin (UCB) and its monoglucuronide (BMG) and diglucuronide (BDG) conjugates in bile. The method can be 'scaled up' for preparative isolation of pure BDG and BMG from pigment-enriched biles. We employed an Altex ultrasphere ODS column in the preparative steps and a Waters  $\mu$ -Bondapak C18 column in the separatory and analytical procedures. Bile pigments were eluted with ammonium acetate buffer, pH 4.5, and a 20 min linear gradient of 60–100% (v/v) methanol at a flow rate of 2.0 ml/min for the preparative separations and 1.0 ml/min for the analytical separations. Bile pigments were eluted in order of decreasing polarity (glucuronide > glucose > xylose conjugates > UCB) and were chemically identified by t.l.c. of their respective ethyl anthranilate azo derivatives. Quantification of UCB was carried out by using a standard curve relating a range of h.p.l.c. integrated peak areas to concentrations of pure crystalline UCB. A pure crystalline ethyl anthranilate azo derivative of UCB (AZO·UCB) was employed as a single h.p.l.c. reference standard for quantification of BMG and BDG. We demonstrate that: (1) separation and quantification of biliary bile pigments are rapid ( $\sim$  25 min); (2) bile pigment concentrations ranging from 1–500  $\mu$ M can be determined 'on line' by using 5  $\mu$ l of bile without sample pretreatment; (3) bilirubin conjugates can be obtained preparatively in milligram quantities without degradation or contamination by other components of bile. H.p.l.c. analyses of a series of mammalian biles show that biliary UCB concentrations generally range from 1 to 17  $\mu$ M. These values are considerably lower than those estimated previously by t.l.c. BMG is the predominant, if not exclusive, bilirubin conjugate in the biles of a number of rodents (guinea pig, hamster, mouse, prairie dog) that are experimental models of both pigment and cholesterol gallstone formation. Conjugated bilirubins in the biles of other animals (human, monkey, pony, cat, rat and dog) are chemically more diverse and include mono-, di- and mixed diconjugates of glucuronic acid, xylose and glucose in proportions that give distinct patterns for each species.

Abbreviations used: UCB, unconjugated bilirubin; BMG, bilirubin monoglucuronide; BDG, bilirubin diglucuronide; IPA, integrated peak area; AZO·UCB, azo derivative of UCB; AZO·CB, conjugated isomeric azo-pigment; BMG-G1, bilirubin monoglucuronide monoglucoside; BMG1, bilirubin monoglucoside; ERCP, endoscopic retrograde cholangiopancreatography; BMX, bilirubin monoxyside; BDG1, bilirubin diglucoside.

\* Present address: Department of Pediatrics, Division of Pediatric Gastroenterology, The New York Hospital-Cornell University Medical Center, 525 East 68th Street, New York, NY 10021, U.S.A.

† To whom correspondence and reprint requests should be addressed at: Department of Medicine, Division of Gastroenterology, Brigham and Women's Hospital, 75 Francis Street, Boston, MA 02115, U.S.A.

In most mammals, bilirubin IX $\alpha$  (bilirubin, UCB) is the major degradation product of haem. Since UCB is insoluble in water at physiological pH (Brodersen, 1979), it is transformed to a family of water-soluble derivatives by hepatic conjugation of one or both of its propionyl groups with glucuronic acid, glucose or xylose (Fevery *et al.*, 1977). Mono- and di-conjugated bilirubins and, apparently, a small amount of UCB, are then secreted into bile (Blanckaert & Schmid, 1982).

Accurate separation and quantification of UCB and its conjugates have proven difficult, since these compounds readily undergo photochemical or oxidative degradation, molecular rearrangements and/or hydrolysis. The ethyl anthranilate diazotization method (Van Roy & Heirwegh, 1968; Fevery *et al.*, 1972; Heirwegh *et al.*, 1974), which converts bilirubins into stable dipyrrolic azo derivatives, has traditionally been employed to separate and measure bilirubin conjugates by t.l.c. and to identify individual conjugating sugars. However, this method may overestimate the levels both of bilirubin monoconjugates (Fevery *et al.*, 1977) and UCB (Gordon *et al.*, 1977) in bile. Moreover, when bilirubin is conjugated with a variety of sugars, it is not possible to determine, from the dipyrrolic derivatives, the original covalent linkages in the native tetrapyrroles.

Alkaline methanolysis followed by t.l.c. (Blanckaert, 1980) or h.p.l.c. (Woolridge & Lightner, 1978; Blanckaert *et al.*, 1980) has also been employed to separate and quantify bilirubin and its conjugates. Although these methods use pure bilirubin methyl ester standards, substitution of methyl groups for the conjugating sugars precludes precise identification of the native bilirubin conjugates. Chowdhury *et al.* (1981, 1982) employed reverse-phase h.p.l.c. to separate and quantify native bilirubins, pure standards of biosynthetically prepared radiolabelled bilirubin conjugates being used. Radiolabelled bilirubin conjugates are difficult and time-consuming to produce and, owing to their chemical instability, they cannot be readily stored. Onishi *et al.* (1980) proposed an 'accurate and sensitive' h.p.l.c. method for analysis of conjugated and unconjugated bilirubins in biological fluids; however, their procedure lacked standards for quantification of conjugated bilirubins and analysis times were  $\approx 100$  min.

To overcome these problems, we have developed a facile and sensitive h.p.l.c. method for on-line separation and quantification of native bile pigments in bile and for preparative isolation of pure BDG and BMG from bilirubin-enriched bile. Crystalline UCB and its crystalline ethyl anthranilate azo derivative are utilized as the sole h.p.l.c. reference standards.

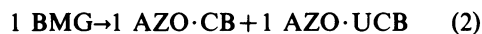
## Theory

The theoretical basis of the method is outlined in Scheme 1 and the details of each step are described in the Procedures and Results section. Our goal was to inject directly a bile sample into the h.p.l.c. column and determine the absolute concentrations of bile pigments from their respective h.p.l.c. integrated-peak-area (IPA) values. The quantification of UCB is straightforward, since crystalline UCB is readily obtained and purified (McDonagh & Assisi, 1971, 1972). Therefore [UCB] can be directly related to its h.p.l.c. IPA (UCB IPA) as shown in step 1 (Scheme 1). There are no crystalline standards commercially available for BMG and BDG; hence the azo derivative of UCB (AZO·UCB) was synthesized and crystallized (step 2, Scheme 1). For the purpose of constructing standard curves, concentrated solutions of BDG and BMG were preparatively isolated by h.p.l.c. from pigment-enriched biles (step 3, Scheme 1). AZO·UCB was employed as the sole standard for determining absolute BMG and BDG concentrations as described below (steps 4 and 5, Scheme 1).

Since both propionyl groups of BDG are conjugated with glucuronic acid, the ethyl anthranilate diazo reaction forms 2 mol of the conjugated isomeric azo-pigments (AZO·CB) for each mol of BDG (step 4, Scheme 1):



BMG contains only one conjugated propionyl group (glucuronic acid at C-8 or C-12); therefore BMG diazotizes to form equimolar proportions of AZO·CB and AZO·UCB (the unconjugated azo pigment) (step 5, Scheme 1):



Since the reactions described in eqns. (1) and (2) go to completion under the appropriate experimental conditions (see the Procedures and results section), then:

$$[\text{BMG}] = [\text{AZO} \cdot \text{CB}] = [\text{AZO} \cdot \text{UCB}] \quad (3)$$

or:

$$[\text{BMG}] = 1/2\{[\text{AZO} \cdot \text{CB}] + [\text{AZO} \cdot \text{UCB}]\} \quad (4)$$

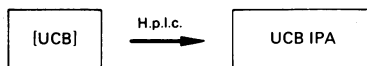
and:

$$[\text{BDG}] = 1/2[\text{AZO} \cdot \text{CB}] \quad (5)$$

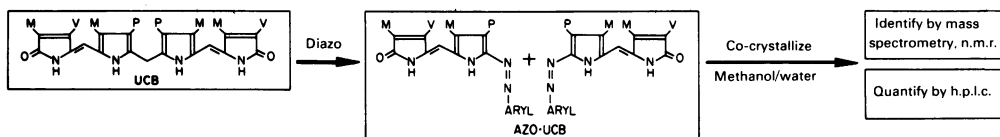
Then a standard curve of [AZO·UCB] against AZO·UCB IPA is constructed to give:

$$[\text{AZO} \cdot \text{UCB}] = f_1(\text{AZO} \cdot \text{UCB IPA}) \quad (6)$$

For a range of unknown BDG concentrations, BDG IPA values ( $\lambda = 450$  nm) and the corresponding AZO·CB IPA values ( $\lambda = 530$  nm) are deter-

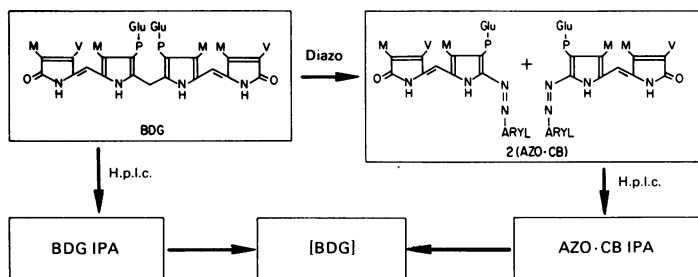
Step 1: Quantification of bilirubin-IX $\alpha$ 

## Step 2: Formation of azo derivative of UCB

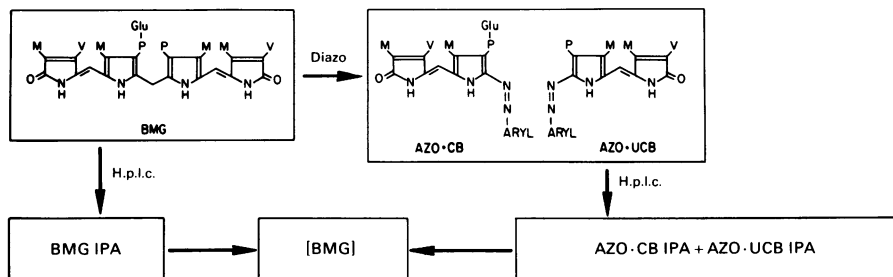


## Step 3: Preparation of pure concentrated BDG and BMG by h.p.l.c.

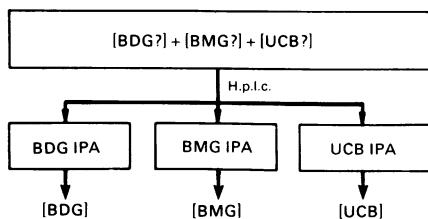
## Step 4: Quantification of BDG by h.p.l.c.



## Step 5: Quantification of BMG by h.p.l.c.



## Analysis of bile sample:



Scheme 1. Overall flow-sheet for h.p.l.c. quantification of unconjugated bilirubin (UCB), bilirubin monoglucuronide (BMG) and bilirubin diglucuronide (BDG) using the ethyl anthranilate azo pigment of UCB (AZO · UCB) and UCB as standards  
See the text for details

mined (step 4, Scheme 1). BDG IPA is then plotted as a function of AZO·CB IPA as follows:

$$\text{BDG IPA} = f_2(\text{AZO} \cdot \text{CB IPA}) \quad (7)$$

Assuming that the relationship between [AZO·UCB] and AZO·UCB IPA is the same as the relationship between [AZO·CB] and AZO·CB IPA, then:

$$[\text{AZO} \cdot \text{CB}] = f_1(\text{AZO} \cdot \text{CB IPA}) \quad (8)$$

$f_1$  having been determined from eqn. (6). The h.p.l.c. IPA of a compound is a function of its solvent composition, molar absorptivity, and concentration. Because the eluting solvent compositions of AZO·CB and AZO·UCB are nearly identical and since glucuronic acid does not change the chromophore of the molecules, the molar absorptivities should be similar. Hence, both AZO·CB and AZO·UCB should have comparable relationships between their concentrations and their IPA values.

From eqns. (5) and (8) and from  $f_1$  of eqn. (6):

$$[\text{BDG}] = \frac{1}{2}\{f_1(\text{AZO} \cdot \text{CB IPA})\} \quad (9)$$

Since we now know [BDG] and the corresponding BDG IPA value, we can plot:

$$[\text{BDG}] = f_3(\text{BDG IPA}) \quad (10)$$

Similarly, for a range of BMG concentrations, BMG IPA and the corresponding AZO·UCB IPA + AZO·CB IPA values are determined (step 5, Scheme 1). From eqns. (4), (6) and (8) we obtain:

$$[\text{BMG}] = f_1\left\{\frac{1}{2}(\text{AZO} \cdot \text{UCB IPA} + \text{AZO} \cdot \text{CB IPA})\right\} \quad (11)$$

Under ideal circumstances, it is possible to determine BMG from AZO·UCB IPA alone, since  $[\text{BMG}] = [\text{AZO} \cdot \text{UCB}] = f_1(\text{AZO} \cdot \text{UCB IPA})$ . However, as we demonstrate in the results, traces of BDG and molecular rearrangement of BMG to form BDG (and UCB) will, in some instances, cause (AZO·CB IPA) to be non-equivalent with (AZO·UCB IPA).

Once [BMG] is known, we can plot:

$$[\text{BMG}] = f_4(\text{BMG IPA}) \quad (12)$$

Finally, once  $f_3$  and  $f_4$  are determined and standard curves for eqns. (10) and (12) are plotted, [BDG] and [BMG] can be determined directly from their respective h.p.l.c. IPA values without recourse to the diazo reaction with each bile sample.

## Experimental

### Materials

**Laboratory animals and bile samples.** Male Sprague-Dawley rats (250–300 g), Duncan-Hartley guinea pigs (250–300 g), and Syrian hamsters (75–125 g) were obtained from Charles River Breeding

Laboratories (Wilmington, MA, U.S.A.). Female prairie dogs (*Cynomys ludovicianus*, ~1 kg) were obtained from Otto M. Locke (New Branfels, TX, U.S.A.). Male and female deer mice (*Peromyscus maniculatus*), homozygous for inherited spherocytosis (*sp/sp*) and the homozygous wild strains (+/+) were obtained from a laboratory colony (courtesy of Dr. Samuel E. Lux, Children's Hospital Medical Center, Boston, MA, U.S.A.). All animals were housed at 24–27°C and allowed free access to appropriate animal chow and water. Diurnal light cycles were 12h on/12h off, beginning at 08:00 and 20:00h respectively.

After an overnight fast, animals were anaesthetized with diethyl ether, and the biliary tree was exposed through a midline abdominal incision. Gall-bladder bile was aspirated *in toto* by hypodermic-needle puncture of the gall bladder. Depending upon the experimental conditions, common-hepatic-duct bile was collected for 30–60 min periods during and after recovery from anaesthesia. Samples of guinea-pig or rat hepatic biles enriched with bilirubin conjugates were obtained via a total bile fistula after infusion of a UCB solution (1 mg/ml, pH ~10.0, 0.05 M-NaOH) into a jugular vein at a rate of 2–3 ml/h.

**Other bile samples.** After appropriate written informed consent and Institutional Human Subjects Committee approval, normal human bile samples were obtained via cannulation of the common bile duct of patients with clinical indications for ERCP. Human hepatic bile samples were obtained 7–8 days after cholecystectomy for gallstones via indwelling T-tube drainage. A gall-bladder bile sample was obtained after cholecystectomy for cholesterol stones. Rhesus-monkey (*Macacca fascicularis*) bile (courtesy of New England Regional Primate Research Center, Southboro, MA, U.S.A.) was obtained by hypodermic-needle puncture of the gall bladder and via a biliary cannula in the common hepatic duct during anaesthesia with ketamine. Bile samples from female Shetland ponies (*Equus caballus*) were obtained from animals fitted with a chronic biliary fistula, and bile samples of cats (*Felis catus*) and dogs (*Canis familiaris*) were obtained by aspirating the gall bladders during diethyl ether anaesthesia (all obtained by courtesy of Dr. Larry R. Engeling, Tufts University School of Veterinary Medicine, Boston, MA, U.S.A.).

**Chemicals.** Crystalline UCB was obtained from Porphyrin Products (Logan, UT, U.S.A.). After recrystallization (McDonagh & Assisi, 1972) the material contained more than 96% of the IX $\alpha$  isomer as determined by t.l.c. (McDonagh & Assisi, 1971) and h.p.l.c. (the present method). Ethyl anthranilate, NaN<sub>3</sub>, n-butyl acetate and pentan-2-one were of reagent grade or American Chem-

ical Society (A.C.S.) quality (Eastman Kodak Co., Rochester, NY, U.S.A.). Reagent- and/or A.C.S.-grade acetic acid, HCl, ammonium hydroxide, acetone and hexane were obtained from Fisher Scientific (Boston, MA, U.S.A.). Reagent-grade ammonium sulphamate, ammonium sulphate,  $\text{NaNO}_3$ ,  $\text{Na}_2\text{EDTA}$ , glycine, Tris base and L-ascorbic acid were all purchased from Sigma Chemical Co. (St. Louis, MO, U.S.A.).  $\text{N}_2$  gas, purity >99.99%, was obtained from Yankee Oxygen (Boston, MA, U.S.A.) and Argon gas, >99.99% pure, was obtained from Matheson Gas Co. (Gloucester, MA, U.S.A.). Water was filtered, deionized and double-distilled through an all-glass apparatus (Corning Glassworks, Corning, NY, U.S.A.) and de-gassed by bubbling with argon.

**Equipment: h.p.l.c. apparatus.** All h.p.l.c. hardware (with exceptions as noted) was purchased from Beckman Instruments (Fullerton, CA, U.S.A.) and included two model 110A pumps, a model 210 sample injector with 5  $\mu\text{l}$ , 100  $\mu\text{l}$  and 250  $\mu\text{l}$  injection loops, a model 410 gradient control board and mixing chamber (all of Altex manufacture), a Hitachi 100-40 variable-wavelength detector, and a Shimadzu CR1A computing integrator. For analytical separations, a Waters  $\mu$ -Bondapak C18 column (Waters Associates, Milford, MA, U.S.A.) (10  $\mu\text{m}$  particle size) with an internal diameter of 3.9 mm and a length of 250 mm was employed. For preparative h.p.l.c., an Altex Ultrasphere ODS column (5  $\mu\text{m}$  particle size) with an internal diameter of 10 mm and a length of 250 mm was used. To protect the columns from possible contamination with bile proteins, each was fitted with a 50 mm Whatman Co: Pell ODS reverse-phase pre-column (Whatman, Clifton, NJ, U.S.A.). Sep-pak C18 cartridges, for sample 'clean-up' before preparative chromatography, were obtained from Waters Associates (Milford, MA, U.S.A.).

**Methods. General Methods.** All experiments were performed in semi-darkness at room temperature (24°C) unless otherwise specified. Before each experiment, standard solutions of UCB and its conjugates were prepared, and between studies were stored on ice under argon. Standard solutions of UCB and its conjugates were discarded if not used within 6 h of their preparation. Native bile samples collected under argon, on ice, in the dark, were analysed by h.p.l.c. within minutes to a few hours of collection. A small number of bile samples that were not analysed within these times were stored at -20°C under argon in tubes containing 5 mM- $\text{Na}_2\text{EDTA}$  and 1 mM-ascorbic acid. Before analysis, all h.p.l.c. solvents and buffers were filtered through 0.1  $\mu\text{m}$ -pore-size Millipore membranes (Millipore Corp., Bedford, MA, U.S.A.) and degassed under reduced pressure for 10–20 min.

Stock buffer solutions were prepared as follows: glycine/HCl buffer was prepared from 0.4 M-HCl adjusted with solid glycine to pH 2.7; ammonium acetate buffer was prepared by titrating 1% (v/v) acetic acid with concentrated (28–30% w/v)  $\text{NH}_4\text{OH}$  to a pH of 4.5; Tris/HCl buffer, pH 9.3, was prepared by the addition of 1 M-HCl to 5 mM-Tris base containing 0.15 M-NaCl and 0.02% (w/v)  $\text{NaN}_3$ .

Measurement of biliary lipids. Cholesterol was measured using a cholesterol oxidase kit (Fromm *et al.*, 1980); total bile salts were measured using the 3 $\alpha$ -steroid dehydrogenase method (Talalay, 1960), as modified by Admirand & Small (1968). Phospholipids were measured by both a choline oxidase kit (Gurantz *et al.*, 1981) and the Bartlett (1959) procedure for inorganic phosphorus.

**Specific methods. Preparation of AZO·UCB.** (1) Ethyl Anthranilate diazo reagent. A freshly prepared 0.25 ml solution of sodium nitrite (100 mg/ml) was added to a fine suspension of ethyl anthranilate (0.05 ml) in 5 ml of 0.15 M-HCl. After vortex-mixing for approx. 5 min to achieve optical clarity, 0.4 ml of ammonium sulphamate (100 mg/ml) was added; vortex-mixing was continued until homogeneity was achieved. For all diazo reactions performed, this ethyl anthranilate diazo reagent was used approx. 3–5 min after its preparation. [The diazo reagent employed in the present work differs from that used by Heirwegh *et al.* (1974), since we found that it was impossible to crystallize AZO·UCB when a large molar excess of ethyl anthranilate was present. It appears that the unchanged oily ethyl anthranilate prevented AZO·UCB from crystallizing.]

(2) Diazotization of UCB. Exactly 467.5 mg of UCB dissolved in 50 ml of 0.1 M-NaOH was added to a continuously stirred 200 ml solution of Tris/HCl buffer, pH 9.3. Over a subsequent 5 min mixing period, 40 ml of the diazo reagent was added dropwise from a burette. After mixing for 20 min, 2.5 ml of ascorbic acid (100 mg/ml) was added and was stirred in for an additional 3 min. The aqueous mixture was then extracted with four successive 300 ml portions of chloroform. If emulsification occurred during the extraction procedure, an excess of anhydrous  $(\text{NH}_4)_2\text{SO}_4$ , an emulsion breaker, was added. The chloroform extract containing AZO·UCB was then washed three times with 300 ml portions of distilled water, pH 6.0, and dried over anhydrous  $(\text{NH}_4)_2\text{SO}_4$ . After 2 h the  $(\text{NH}_4)_2\text{SO}_4$  was removed by filtration.

(3) Crystallization of AZO·UCB. The chloroform/AZO·UCB extract was dried by rotary evaporation at 50–55°C. Precipitated AZO·UCB was dissolved in a few millilitres of methanol and, during cooling on ice, a small portion of crushed ice

was added. If crystallization did not begin within a few minutes, more crushed ice was added and the side of the test tube was scratched with a glass rod. Approx. 2h after crystallization the solution was filtered through a fine sintered-glass filter and the purple crystals of AZO·UCB were washed with a few millilitres of cold (4°C) reagent-grade acetone. From the filtrate the remaining AZO·UCB was recrystallized twice, giving an overall yield of 65%. T.l.c. of 200 µg of the crystalline azo pigments on silica-gel G [solvent system: chloroform/methanol, 17:3 (v/v)] (Heirwegh *et al.*, 1974) revealed a single spot. H.p.l.c. on a Waters µ-Bondapak C18 analytical column (method described below) gave a single elution peak. H.p.l.c. on an Altex ultrasphere ODS analytical column, with a linear aqueous-methanol gradient (see the subsection below) separated the azo pigments into approximately equal amounts of vinyl and isovinyl isomers. This separation allowed us to determine that both isomers were present, but this step was not necessary for bile-pigment quantification. The mass spectra and the proton n.m.r. of these compounds corresponded exactly to previously reported spectra (Compernelle *et al.*, 1970, 1980).

T.l.c. and h.p.l.c. peak identification. Individual peaks of conjugated bilirubins from preparative and analytical h.p.l.c. columns were collected,

diazotized with ethyl anthranilate and identified by t.l.c. by the method of Heirwegh *et al.* (1974). The diazo products of bile pigments from the dog were employed as reference t.l.c. standards.

H.p.l.c. elution. Before each separation, the h.p.l.c. column was equilibrated for 5 min with methanol/ammonium acetate buffer, pH 4.5, (3:2, v/v) at a flow rate of 2 ml/min. At the time of sample injection, a 20 min linear gradient of 60→100% (v/v) methanol in 1% ammonium acetate buffer was initiated. For analytical separations of UCB and its conjugates, the column flow rate was 1.0 ml/min and the injector-loop volume was 5 µl. For preparative operation and isolation of bilirubin conjugates, the column flow rate was 2 ml/min, and the injector-loop volume was 100–250 µl.

## Procedures and results

### Quantification of UCB (step 1 of Scheme 1)

To prepare a standard curve, a freshly prepared stock solution of UCB (5.84 mg in 10 ml of 0.1 M-NaOH) was diluted with methanol to give final UCB concentrations that ranged from 2.5 to 50 µM. Each concentration was injected three times into the Waters µ-Bondapak C18 analytical column and the mean IPA of UCB was determined at  $\lambda = 450$  nm. As depicted in Fig. 1, a plot of UCB

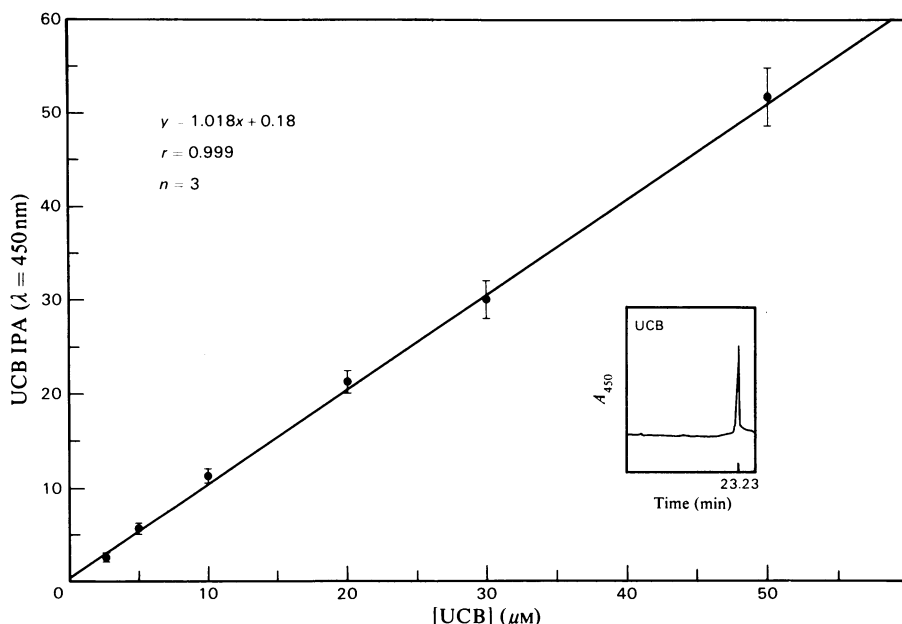


Fig. 1. Dependence of h.p.l.c. integrated peak area (IPA) of UCB (UCB IPA) (in arbitrary units,  $\times 10^{-3}$ ) on [UCB]. The inset shows typical h.p.l.c. elution peak of UCB (retention time 23.23 min) measured as  $A_{450}$ . UCB concentrations ranging from 2.5 to 50 µM were injected into a Waters µ-Bondapak C18 analytical column and eluted with a linear gradient of methanol and ammonium acetate, pH 4.5. The corresponding IPA values were measured at  $\lambda = 450$  nm. Each point represents the mean IPA for three h.p.l.c. injections and the vertical bars represent  $\pm 1$  S.D.

IPA against [UCB] in  $\mu\text{M}$  was linear. The inset (Fig. 1) shows a typical h.p.l.c. elution profile of UCB at time ( $t$ ) = 23.23 min, measured as absorbance ( $A$ ) at 450 nm.

#### Quantification of AZO·UCB (step 2 of Scheme 1)

A 1 mM stock solution of AZO·UCB (4.62 mg) was prepared in 10 ml of pentan-2-one. The solution was further diluted (with pentan-2-one) to give AZO·UCB concentrations that ranged from 5 to 500  $\mu\text{M}$ . Each concentration was injected three times into the Waters  $\mu$ -Bondapak C18 analytical column and the mean IPA of AZO·UCB was determined at  $\lambda = 530$  nm. As Fig. 2 shows, a plot of AZO·UCB IPA against [AZO·UCB] was also linear. The inset shows a typical h.p.l.c. elution profile of AZO·UCB at retention time ( $t$ ) = 22.56 min measured as absorbance ( $A$ ) at 530 nm.

#### Preparation of pure BDG and BMG (Step 3 of Scheme 1)

Immediately after collection on ice, 100  $\mu\text{l}$  of bilirubin-enriched rat bile was diluted 1:2 (v/v) with 1% acidified methanol (1 ml of acetic acid in 100 ml of methanol). The solution was gently vortex-mixed and then centrifuged for 2 min on a Microfuge. The supernatant was aspirated and 100–250  $\mu\text{l}$  was injected into the Altex Ultrasphere ODS preparative column. Alternatively, pigment-enriched rat bile can be applied directly to a Sep-pak C18 cartridge pre-washed with 1% acidified methanol and the pigments eluted with 2 ml of the same solvent. In the presence of alkaline bile, the addition of acetic acid is necessary to prevent methanolysis of the pigments. Before h.p.l.c. injection, the methanolic solution was evaporated under  $\text{N}_2$  at 27°C. The first major pigment was eluted in approx. 13 min and the second major pigment was eluted in 19 min; diazo analysis of the

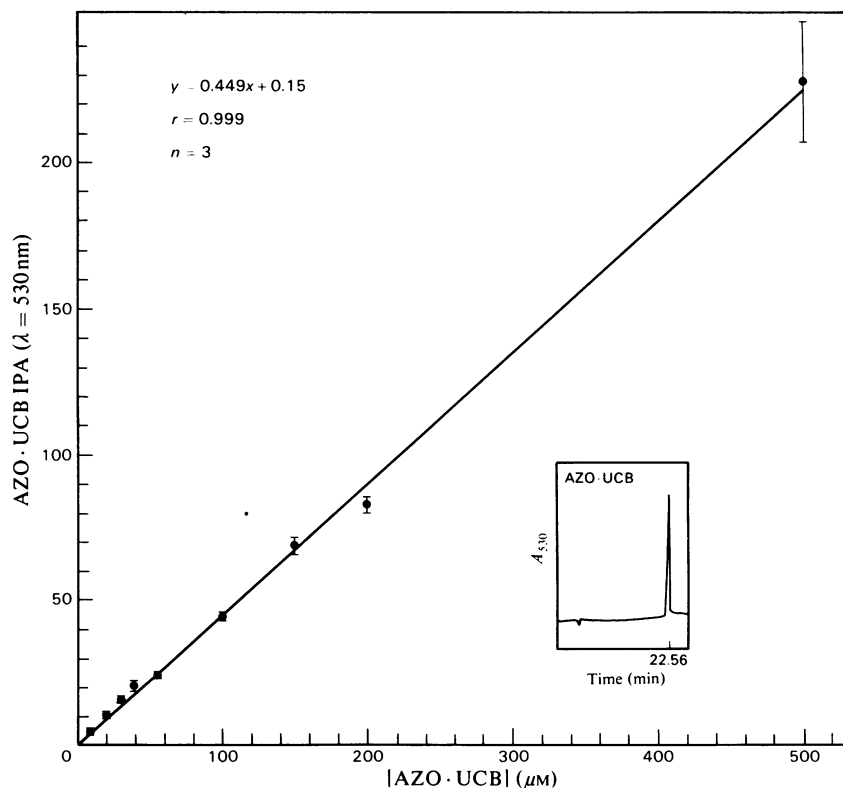


Fig. 2. Dependence of h.p.l.c. IPA of AZO·UCB (AZO·UCB IPA) (in arbitrary units,  $\times 10^{-3}$ ) on [AZO·UCB]. The inset shows typical h.p.l.c. elution peak of AZO·UCB (retention time, 22.56 min) at  $\lambda = 530$  nm. Crystalline AZO·UCB was diluted in pentan-2-one to give final concentrations of 5–500  $\mu\text{M}$ . Each point on the curve represents the mean IPA for three h.p.l.c. injections and bars represent  $\pm 1$  s.d. The formula to determine [AZO·UCB] is:

$$f_1(y) = 2.23x - 0.33.$$

two fractions indicated that these were BDG and BMG respectively. If desired, pure BMG and BDG can be prepared without contamination with ammonium acetate, water or methanol, by one of the following methods: (1) The h.p.l.c. pigment eluates are concentrated under  $N_2$  at  $27^\circ C$  to a final volume of  $100 \mu l$ . Concentrated pigment solutions are then individually applied to a Sep-pak C18 cartridge prewashed with distilled water. Solutions are then washed on a Sep-pak cartridge with 3 ml of distilled water to remove ammonium acetate and eluted separately with 100% (v/v) methanol followed by evaporation of the methanol under  $N_2$ . (2) The h.p.l.c. separation is performed with an aq. 1% ammonium formate buffer and a 65–100% 20 min linear gradient of methanol. Methanol is removed under  $N_2$  at  $27^\circ C$ , and water and ammonium formate are removed by freeze-drying. The residue is the pure bile pigment as determined by analytical h.p.l.c. and chemical analysis.

#### Quantification of BDG (step 4 of Scheme 1)

Aqueous-methanol solutions containing pure BDG isolated from the preparative h.p.l.c. column were evaporated under  $N_2$  to near-dryness at  $24^\circ C$ . Each pigment fraction was then dissolved in an appropriate volume of distilled water, pH 6.0, and divided into two portions. The first portion was injected into the Waters  $\mu$ -Bondapak C18 analytical column and the IPA at 450 nm was measured. To the other portion,  $50 \mu l$  of pentan-2-one,  $50 \mu l$  of glycine buffer and  $50 \mu l$  of diazo reagent were added in sequence. The diazotized BDG mixture was vortex-mixed for 30 s at zero time, 10 min and 20 min. At 30 min, h.p.l.c. elution of the diazo mixture scanned at  $\lambda = 450 \text{ nm}$  indicated that the diazo reagent had completely reacted with all BDG present. At this time the diazo mixture was centrifuged on a Microfuge for 2 min, the pentan-2-one layer was immediately injected into a Waters  $\mu$ -Bondapak C18 analytical column and the IPA of the azo derivative (AZO·CB) was measured at  $\lambda = 530 \text{ nm}$ . As Fig. 3 shows, a linear standard curve was then constructed to relate AZO·CB IPA to BDG IPA. The insets show the h.p.l.c. elution profiles of AZO·CB at  $t = 19.77 \text{ min}$  and BDG at  $t = 9.52 \text{ min}$  measured as absorbance ( $A$ ) at 530 nm and 450 nm respectively. The right ordinate gives [BDG], which is determined as follows.

First,  $f_1(\text{AZO} \cdot \text{UCB IPA})$  from eqn. (6) is equal to  $f_1(y)$  in Fig. 2 (see the legend):

$$f_1(y) = 2.23x - 0.33 \quad (13a)$$

Secondly, the function  $f_1$  is then applied to AZO·CB IPA (from Fig. 3) as in eqn. (9):

$$\begin{aligned} [\text{BDG}] &= \frac{1}{2}[\text{AZO} \cdot \text{CB}] \\ &= \frac{1}{2}\{2.23(\text{AZO} \cdot \text{CB IPA}) - 0.33\} \quad (13b) \end{aligned}$$

Thirdly, since AZO·CB IPA can be expressed as a function of BDG IPA (Fig. 3), then:

$$[\text{BDG}] = 1.115(1.066 \text{ BDG IPA} + 6.24) - 0.16 \quad (13c)$$

and, finally, as in Fig. 3:

$$[\text{BDG}] = 1.188(\text{BDG IPA} + 6.88) \quad (13d)$$

#### Quantification of BMG (step 5 of Scheme 1)

Whereas BDG is relatively stable in bile and can also be stored in organic solvents at  $-20^\circ C$  for as long as 3 days, BMG in aqueous solution (Jansen, 1973), native bile or organic solvents has a tendency to rearrange spontaneously to BDG and UCB. This spontaneous isomerization forms III $\alpha$  and XIII $\alpha$  isomers of BDG and UCB in addition to the native IX $\alpha$  isomers (Sieg *et al.*, 1982). Storage of pure BMG at  $-20^\circ C$  with subsequent defrosting and warming at  $24^\circ C$  led to variable amounts of molecular rearrangements with the formation of BDG and UCB from BMG. Fig. 4 demonstrates that incubation of aqueous-methanol solutions of pure BMG for 10–30 min at  $40^\circ C$  results in a decrease in the percentage of BMG and an increase in the percentage of BDG and UCB, which form during the molecular rearrangement. The splitting of the UCB peak (Fig. 4) represents III $\alpha$  and XIII $\alpha$  isomers (McDonagh & Assisi, 1971, 1972).

In an attempt to prevent BDG formation from BMG during h.p.l.c. quantification, BMG solutions were evaporated at  $24$ – $27^\circ C$  under a steady stream of argon and BMG was utilized on the day of isolation and kept on ice up to the time of h.p.l.c. injection or diazotization. Thus, under ideal conditions, when BMG is processed for quantification exactly as described for BDG in the section above, the diazo reaction goes to completion and equimolar amounts of AZO·CB and AZO·UCB are formed, as shown by the upper inset to Fig. 5. Nevertheless, under most experimental circumstances, a small portion of standard BMG rearranges to form BDG; the diazo reaction of this BMG and BDG mixture will lead to an excess of AZO·CB. Consequently, it became necessary to derive a more complex relationship between the IPA values of AZO·UCB and AZO·CB, and BMG IPA as shown in Fig. 5. This relationship encompasses all possible degrees of spontaneous isomerization and is based on the following considerations.

If a sample contains only BDG or BMG, accurate quantification follows from eqns. (9) and (11) respectively. Therefore, in samples that contain BMG and a small amount of BDG



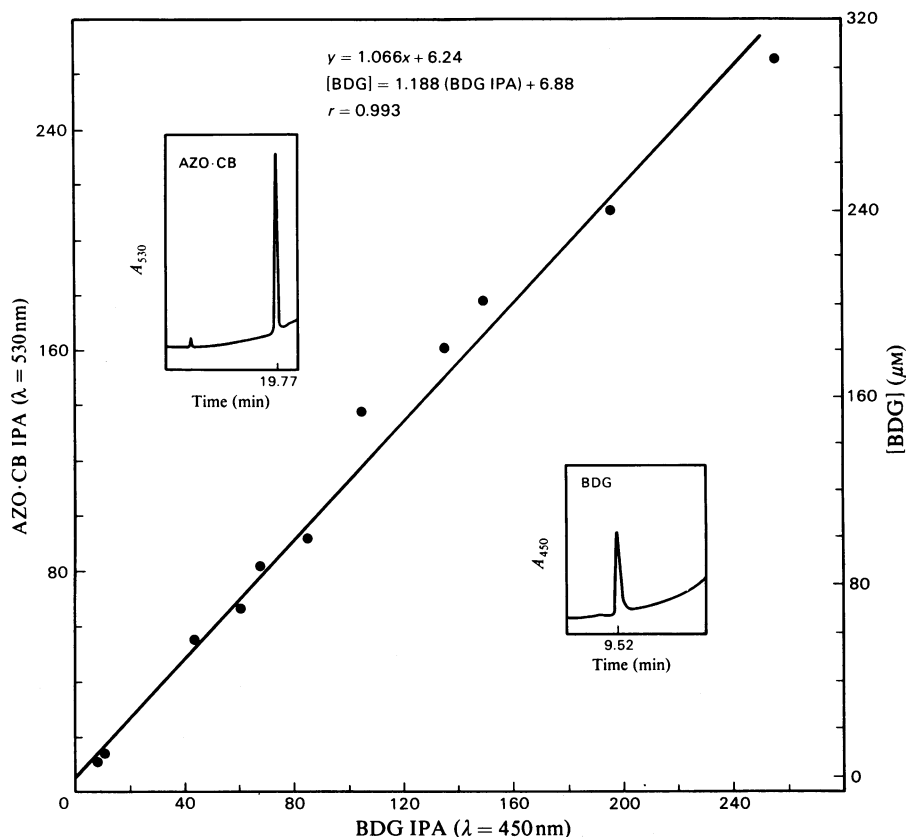


Fig. 3. Plot used for determining [BDG] from BDG IPA

The insets show h.p.l.c. absorbance peaks and retention times for AZO·CB ( $\lambda = 530\text{ nm}$ ) and BDG ( $\lambda = 450\text{ nm}$ ). Pure BDG obtained preparatively by h.p.l.c. was diluted with an appropriate amount of water (pH  $\sim 6.0$ ) and divided into two portions. The IPA of one portion was directly measured on the h.p.l.c. analytical column at  $\lambda = 450\text{ nm}$  (right insert). The other portion was diazotized (AZO·CB) and its h.p.l.c. IPA was measured at  $\lambda = 530\text{ nm}$  (left insert). Each point represents a value for BDG IPA (abscissa) and its corresponding AZO·CB IPA (left ordinate) for an individual concentration of BDG. Since the molar absorptivities of AZO·CB and AZO·UCB are virtually identical (see Fig. 5, inset), the AZO·CB IPA values on the left ordinate can be read as 'AZO·UCB IPA'. By using the relationship for  $f_1(y)$  in the legend to Fig. 2, the AZO·CB IPA values are converted into [AZO·CB], from which [BDG] on the right ordinate is obtained according to eqns. 13a, 13b, 13c and 13d).

(<20  $\mu\text{M}$ ), we combine eqns. (9) and (11) to obtain:

$$[\text{BMG}] + [\text{BDG}] = f_1 \left\{ \frac{1}{2} (\text{AZO} \cdot \text{UCB IPA} + \text{AZO} \cdot \text{CB IPA}) \right\} \quad (14a)$$

From eqn. (13d) [for small values of BDG IPA in the range of  $(5-10) \times 10^{-3}$  arbitrary units]:

$$[\text{BDG}] = f_1(\text{BDG IPA}) \approx 2.23(\text{BDG IPA}) \quad (14b)$$

Then:

$$[\text{BMG}] = f_1 \left\{ \frac{1}{2} (\text{AZO} \cdot \text{UCB IPA} + \text{AZO} \cdot \text{CB IPA}) - \text{BDG IPA} \right\} \quad (14c)$$

In Fig. 5 this corrected IPA value,  $\frac{1}{2}(\text{AZO} \cdot \text{UCB IPA} + \text{AZO} \cdot \text{CB IPA}) - \text{BDG IPA}$ , is plotted on

the left ordinate. [BMG] was solved for in a similar fashion to [BDG] (eqns. 13a, 13b, 13c and 13d above) and plotted on the right ordinate of Fig. 5 as functions of BMG IPA and eqn. 14c.

#### Purity of isolated BDG and BMG

By lipid analysis (see under 'Methods'), neither BMG- nor BDG-containing fractions were contaminated with detectable amounts of cholesterol, bile salts or phospholipids. Proteins of bile were denatured with methanol of the mobile phase and appeared to precipitate completely in the pre-column. For this reason, and especially with daily use, a change of the pre-column every 1-2 months was necessary.

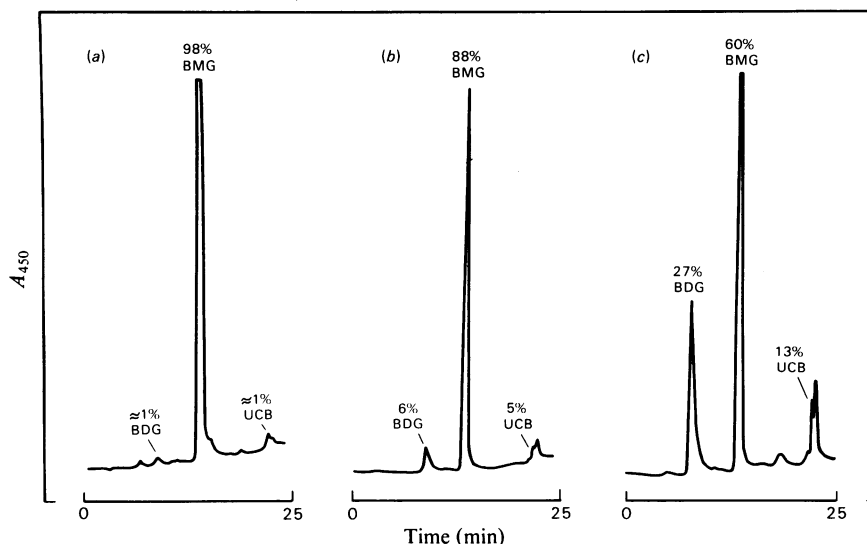


Fig. 4. Time-dependence of molecular rearrangement of BMG to BDG and UCB [ $2 \text{ BMG (IX}\alpha) \rightarrow 1 \text{ BDG} + 1 \text{ UCB (III}\alpha, \text{IX}\alpha, \text{XIII}\alpha)$ ] as evaluated by h.p.l.c.

(a) Typical h.p.l.c. elution profile of 'pure' BMG on a Waters  $\mu$ -Bondapak C18 analytical column after isolation from an Altex preparative column. Sample was concentrated at 25°C under  $\text{N}_2$  before injection. Note that (a) contains 98% BMG with  $\sim 1\%$  BDG and  $\sim 1\%$  UCB. (b) H.p.l.c. elution profile of 'pure' BMG after incubation under  $\text{N}_2$  in aqueous methanol for 10 min at 40°C. (c) H.p.l.c. elution profile of same sample as in (b), but with incubation under  $\text{N}_2$  in aqueous methanol for 30 min at 40°C. Of the total pigments present, the percentage concentration of BMG decreases from 98% (a) to 88% (b) to 60% (c), whereas the percentage concentration of BDG/UCB increases to 6/5% in (b), and 27/13% in (c). The BMG peak in (c) appears larger than the BMG peak in (b), since the sample has been concentrated during heating. Some loss of pigment during the heating process may account for the fact that [BDG] is not equal to [UCB].

During these studies, we discovered that the choline oxidase method (Gurantz *et al.*, 1981) consistently suggested that a choline-containing phospholipid was present in an approximate 1:1 molar ratio with either pure BMG, or even when pure BMG was bleached with u.v. light before enzymic determination. Since the Bartlett (1959) method for inorganic phosphorus detected no phosphorus in these samples, we conclude that both native and 'bleached' BMG give a false-positive test with the choline oxidase method for choline-containing phospholipids. Since most animal biles contain BMG (see below), the choline oxidase method may introduce a variable error in phospholipid determination in bile samples. In the present work the chemistry of this false-positive reaction was not investigated further.

#### Pigment binding to h.p.l.c. columns

One potential problem with direct h.p.l.c. injection of native bile is that bile proteins that precipitate in the precolumn or possibly in the analytical column may bind bile pigments and result in falsely low values for UCB, BMG, and BDG. To test this possibility, we mixed known

amounts of UCB (concentrations determined gravimetrically) and pure BDG (concentrations first determined by h.p.l.c.) with guinea-pig bile samples that contained BMG as the sole bile pigment (see below). Concentrations of pigment were determined by h.p.l.c. before and after addition of exogenous pigment to the samples. As shown in Fig. 6, there was excellent correlation between h.p.l.c.-derived concentrations and concentrations assayed by serial dilution. The complete recovery strongly suggests that bile-pigment precipitation did not take place in the analytical columns and confirms that no tightly (covalently?) bound bilirubin-albumin complexes (Weiss *et al.*, 1983) exist in native bile as demonstrated previously (Kuenzle *et al.*, 1966a,b).

#### Pigment analysis of animal bile samples

Fig. 7 depicts the application of this h.p.l.c. separation and quantification technique to bile samples from a number of rodents (deer mice, prairie dogs, guinea pigs and hamsters), all of which have been studied as experimental models of pigment gallstone formation (Okey, 1944; Anderson *et al.*, 1966; DiFilippo & Blumenthal,

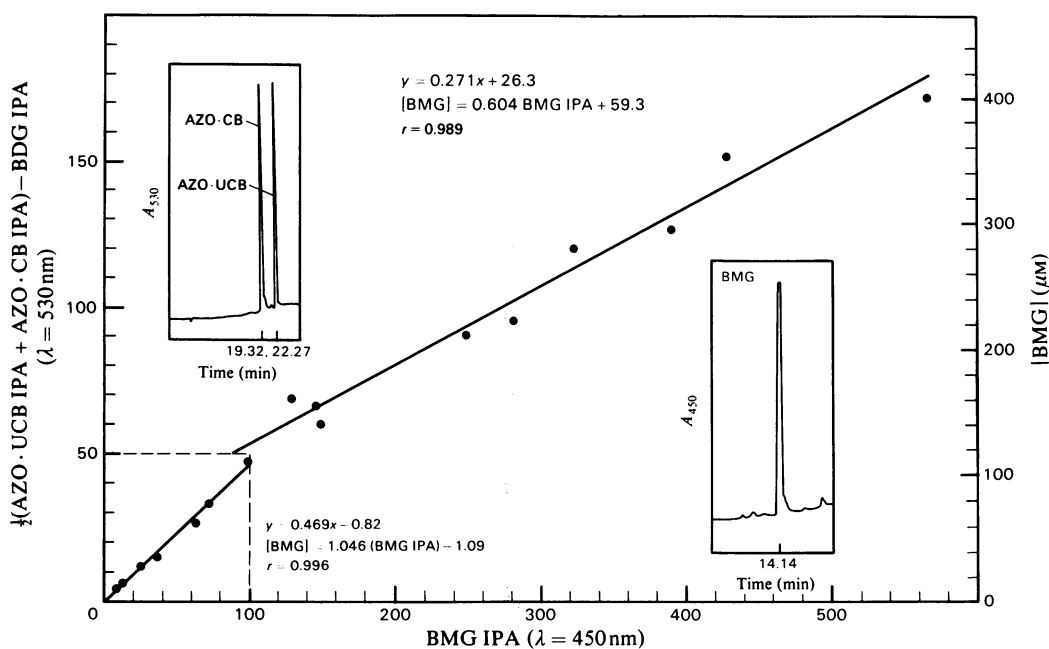


Fig. 5. Plot used for determining [BMG] from BMG IPA

Plot in the box bounded by broken lines is for BMG IPA values  $< 100$  (arbitrary units,  $\times 10^{-3}$ ). Major plot is for BMG IPA values  $> 100$  (arbitrary units,  $\times 10^{-3}$ ). Insets show h.p.l.c. absorbance peaks and retention time for AZO·CB+AZO·UCB ( $\lambda = 530\text{nm}$ ) and BMG ( $\lambda = 450\text{nm}$ ). Pure BMG was obtained preparatively by h.p.l.c., diluted with an appropriate amount of distilled water (pH  $\sim 6.0$ ) and divided into two portions. One portion was directly injected into the analytical h.p.l.c. column and its IPA was measured at  $\lambda = 450\text{nm}$ . The other portion was diazotized and the diazo products (AZO·CB+AZO·UCB) were injected and their individual IPA values were measured at  $\lambda = 530\text{nm}$ . To correct for the unavoidable formation of small amounts (usually  $< 5\%$ ) of BDG formed in each BMG sample (see the text), each point represents the BMG IPA plotted against the corresponding  $\frac{1}{2}(\text{AZO}\cdot\text{UCB IPA} + \text{AZO}\cdot\text{CB IPA}) - \text{BDG IPA}$  for that point. The derivation of  $\frac{1}{2}(\text{AZO}\cdot\text{UCB IPA} + \text{AZO}\cdot\text{CB IPA}) - \text{BDG IPA}$  and theoretical basis for the break point in the standard curve of  $\sim 100$  BMG IPA units are described in the text. By using the relationship in the legend to Fig. 2, the IPA values on the left ordinate were used to give [BMG].

1972; Pitt *et al.*, 1983). These animals secrete BMG as the predominant, if not exclusive, bile pigment. However, the rat, which is not known to form pigment stones, excretes appreciable quantities of BDG in addition to BMG (Fig. 7). As shown in Fig. 8, dog, pony, monkey, cat and human biles all contain a complex pattern of bile pigments. On the basis of t.l.c. of the ethyl anthranilate derivatives (Heirwegh *et al.*, 1974) of dog bile, we have separated ten pigment peaks by h.p.l.c. (Fig. 8), which were employed as reference standards. In Table 1, each dog bile peak is listed in order of decreasing polarity and, with the exception of no. 7, all have been chemically identified. According to this nomenclature, the concentrations (in  $\mu\text{M}$ ) and percentage concentration of bilirubin and its conjugates (identified using the key to Table 1) in various animal biles under a variety of pathophysiological conditions are shown in Tables 2-4.

Table 2 lists animal biles containing predom-

antly BDG and BMG. Some animal biles contain small amounts of other conjugates, particularly BMG-G1 (rat), BMG1 (deer mouse) and BMX (prairie dog, hamster and rat). The concentration of UCB was variable, ranging from 0 (guinea pig) to 10% (anaesthetized rat) of total bile pigments. Whereas total bilirubin concentrations were elevated in *sp/sp* deer mice, only small elevations of [UCB] were observed (Table 2). Further, a hamster with a pigment gallstone showed no major alteration in bile-pigment pattern (Table 2). Table 3 lists animal bile samples containing appreciable amounts of mixed conjugates of bilirubin with glucuronide, glucose and xylose. Although the dog contains all ten conjugates (see Fig. 8), the principal bile pigments in this species are BMG-G1 with lesser amounts of BDG and BMG. In the pony the principal bile pigments are BMG-G1 and BDG1; in the cat the principal bile pigments are BDG and BMG-G1, and in the rhesus monkey the

Table 1. Key to h.p.l.c. elution profiles of mammalian bile pigments in order of decreasing polarity

Peak no.	Abbreviation	Identification of bilirubin conjugate
1	BDG	Diglucuronide
2	BMG-G1	Monoglucuronide monoglucoside
3	BDG1	Diglucoside
4*	BMG-MX	Monoglucuronide monoxyloside
5	BMG1-MX	Monoglucoside monoxyloside
6	BMG	Monoglucuronide
7	—	Unknown
8	BMG1	Monoglucoside
9	BMX	Monoxyloside
10	UCB	Unconjugated bilirubin

\* Peak not actually identified by diazo reaction, but identification based on polarity of sugar and peak elution position.

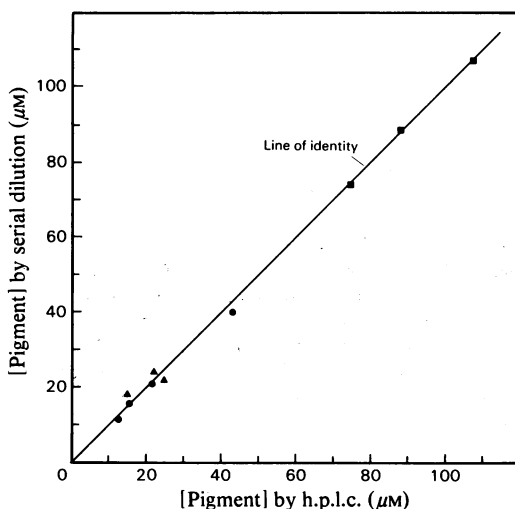


Fig. 6. Plot of bile-pigment (UCB, BMG and BDG) concentrations ( $\mu\text{M}$ ) by serial dilution of bile versus bile-pigment concentrations ( $\mu\text{M}$ ) by h.p.l.c.

The line of identity ( $y = x$ ) provides a best fit for all data points. For UCB ( $\bullet$ ), sets of values were obtained by adding known concentrations of UCB (determined gravimetrically) to guinea-pig bile samples and determining concentrations of added pigment by h.p.l.c. according to the standard curve in Fig. 1. For BDG ( $\blacksquare$ ) and BMG ( $\blacktriangle$ ), initial concentrations in rat bile were derived by h.p.l.c. according to Figs. 3 and 5 respectively, and serial dilutions were then performed. Each data point represents the h.p.l.c.-determined concentration versus the known concentration determined by the dilution factor.

(see Table 1 and Fig. 8), were identified. BDG and BMG are the predominant bile pigments in human beings and are present in ratios that vary from 1.6:1 to 9:1. It is notable that, in all human bile samples, including a patient with a pigment stone and one with a cholesterol stone, the percentage of UCB did not exceed 1% of total bile pigments. The percentage of monoconjugates to total conjugated bilirubin present in human bile varied from a low value of 10.1% in T-tube bile to 33.3% in ERCP bile. As might be expected, the total bilirubin concentration is higher in gall-bladder bile ( $\sim 4\text{mM}$ ) than in hepatic biles.

With regard to the uncommon conjugates, we assumed in these calculations that the molar absorptivities for the xylose and glucose monoconjugates were the same as those for BMG, and the molar absorptivities for all the diconjugates were the same as those for BDG. This assumption is analogous to the approximation made by Heirwegh *et al.* (1974). Those authors assumed that all ethyl anthranilate azo derivatives of bile pigments have the same absorbances regardless of their differing sugar groups. However, specific conjugating sugars may induce minor differences in the molar absorptivities of these compounds. Since in the present work the h.p.l.c. absorbance of each compound was determined in a slightly different percentage of methanol, these variations will only marginally affect the molar absorptivities measured. Nevertheless, the derived concentrations of the uncommon bilirubin conjugates will not be as precise as those for BMG and BDG.

## Discussion

principal bile pigments are BDG, BMG-G1 and BMG. UCB constituted less than 3% of all bile pigments in these animals. Table 4 lists the pigment pattern and concentrations in non-infected human bile samples. All bile pigments found in the dog, with the exception of nos. 4 and 7

The h.p.l.c. method described in the present paper has the merits of simplicity, specificity and technical ease in determining the concentrations of UCB, BMG, and BDG as native tetrapyrroles in bile. It offers the distinct advantage of direct, small-sample ( $5\mu\text{l}$ ) injection without prior precipi-

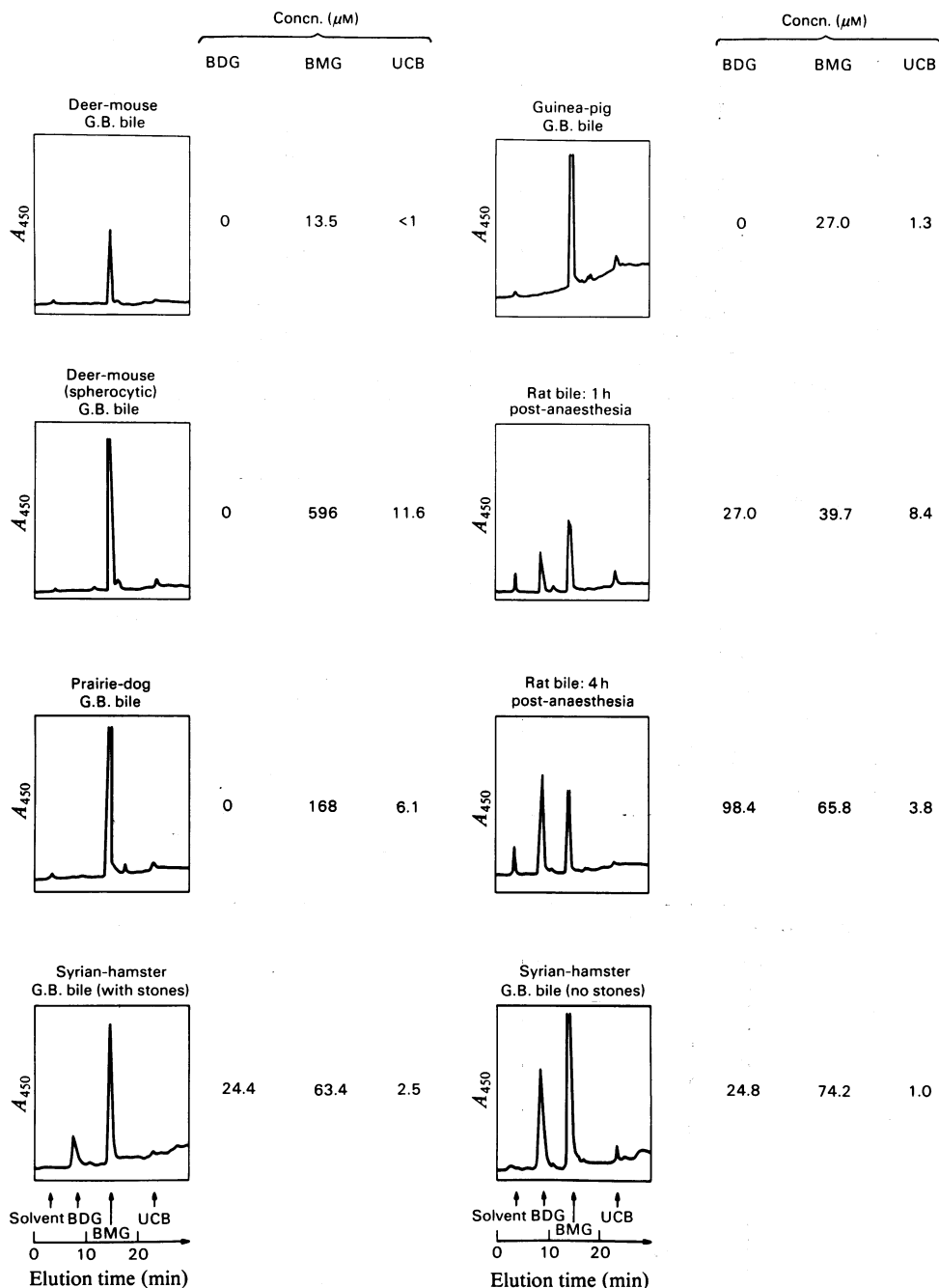


Fig. 7. Typical h.p.l.c. elution profiles and pigment concentration for a variety of rodent bile samples containing predominantly **BMG and BDG**

Bile samples ( $5\ \mu\text{l}$ ) were injected directly into the h.p.l.c. column and concentrations were determined from standard curves (Figs. 1–3 and 5) by converting integrated peak areas (IPA) to pigment concentrations. Deer mouse and rat bile scans are displayed at four times the attenuation and prairie-dog bile is displayed at twice the attenuation of the guinea-pig bile scan. The concentrations of BMG and UCB in the spherocytic-deer-mouse gall bladder (G.B.) bile are severalfold higher than the values for the normal deer mouse. One Syrian-hamster bile contained a pigment stone and was diluted 1:2 (v/v) before h.p.l.c. injection (see Table 2 for analysis).

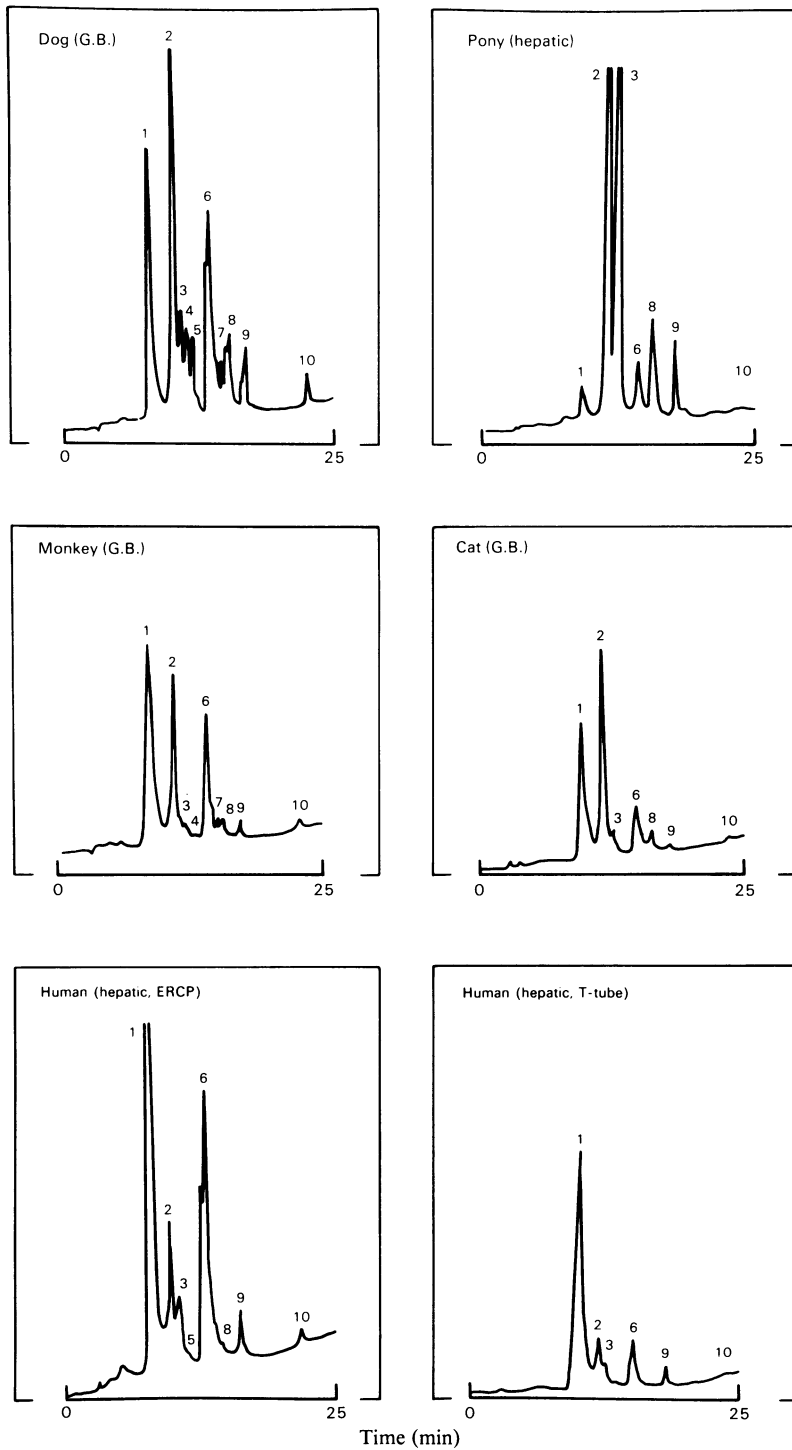


Fig. 8. Typical h.p.l.c. elution profiles of a variety of bile samples containing a variable mixture of bilirubin conjugates in addition to BMG and BDG

Stored bile samples were diluted 1:1 with 5 mM- $\text{Na}_2\text{EDTA}$ /1 mM-ascorbic acid. Gall-bladder (G.B.) bile was further diluted with distilled water (pH  $\sim$ 6.0) 1:20–1:50 (v/v) before h.p.l.c. injection. After rapid thawing, 5  $\mu\text{l}$  of diluted bile was injected into the h.p.l.c. analytical column. Identification of unknown peaks was by means of the ethyl anthranilate diazo reaction and t.l.c. of the derivatives (Heirwegh *et al.*, 1974) (see Tables 3 and 4 for analysis).

Table 2. Animal biles containing predominantly BDG and BMG  
Peak no. on chromatogram is based on elution sequence for dog bile\*.

Animal	Genotype	Site	Gallstones	Notes	Peak no. ... Conjugate	[Bilirubin] ( $\mu\text{M}$ )					Total
						1 BDG	2 BMG-G1	6 BMG	8 BMG1	9 BMX	
Rat		Hepatic	—	1 h† post-op 4h	27.0† (34.7)	2.8 (3.6)	39.7 (51.0)	n.d.§	n.d.	8.4 (10.8)	77.9
		Hepatic	—	post-op	98.4 (57.1)	2.6 (1.5)	65.8 (38.1)	n.d.	1.7 (1.0)	3.8 (2.2)	172.3
Deer mouse	<i>sp/sp</i>	G.B.¶	+		n.d.	n.d.	1160.0 (91.6)	82.9 (6.5)	3.8 (0.3)	20.0 (1.6)	1266.7
	<i>sp/sp</i>	G.B.	+		n.d.	n.d.	596.0 (96.5)	9.8 (1.6)	n.d.	11.6 (1.9)	617.4
	<i>sp/sp</i>	G.B.	+	see (**)	n.d.	n.d.	— (91.3)	n.d.	n.d.	— (8.7)	
	<i>sp/sp</i>	G.B.	—	<i>n</i> = 3	n.d.	n.d.	425.9 ± 185.5 (95.2 ± 1.9)	9.0 ± 11.5 (2.1 ± 1.5)	n.d.	10.5 (3.0 ± 1.7)	445.4 ± 188.0
	<i>sp/sp</i>	Hepatic	+		n.d.	n.d.	300.2 (95.6)	5.2 (1.7)	n.d.	7.8 (2.4)	313.2
	<i>sp/sp</i>	Hepatic	+		n.d.	n.d.	268.8 (95.6)	4.9 (1.7)	n.d.	3.6 (1.2)	277.3
	+/+	G.B.	—		n.d.	n.d.	98.7 (91.2)	3.7 (3.4)	n.d.	5.8 (5.3)	108.2
	+/+	G.B.	—		n.d.	n.d.	13.5 (99)	n.d.	n.d.	<1 (<1%)	14.0
Guinea pig		G.B.	—	Mean <i>n</i> = 6 see ††	n.d.	n.d.	25.5 ± 14.9 (98.1)	n.d.	n.d.	0.5 ± 0.5 (1.9)	26.0 ± 15.4
		Hepatic	—	Mean <i>n</i> = 3	n.d.	n.d.	26.8 ± 9.5 (100)	n.d.	n.d.	n.d.	26.8 ± 9.5
Prairie dog		G.B.	—		n.d.	n.d.	167.8 (95.0)	tr	2.8 (1.6)	6.1 (3.4)	176.7
Hamster		G.B.	+		24.4 (26.8)	tr	63.4 (69.7)	n.d.	0.7 (0.9)	2.5 (2.7)	91.0
		G.B.	—		24.8 (24.6)	tr	74.2 (73.6)	n.d.	0.7 (0.7)	1.0 (1.0)	100.7

\* See Table 1 for peak number and bilirubin symbol identification. Peaks 3, 4, 5, and 7 observed in bile of the domestic dog were not detected, or were below the detectable limits, in rodent biles.

† Time after cessation of diethyl ether anaesthesia.

‡ Values in parentheses are percentage concentrations. Numbers above parentheses are concentrations in  $\mu\text{M}$ .

§ n.d., not detected or below measurable limits of 0.5  $\mu\text{M}$ .

|| *sp/sp*, homozygous spherocytic; +/+, homozygous wild-type.

¶ G.B., gall bladder; other abbreviations: post-op, post-operative; tr, trace.

\*\* Since the volume of bile was less than 5  $\mu\text{l}$  in this gall bladder, the exact volume could not be accurately measured and the concentration could not be calculated. Thus only the relative percentage concentrations are given.

†† The values in this line are means  $\pm$  s.d. for six animals. Thus the values for guinea-pig gall-bladder bile do not match those of Fig. 7, which is for an individual animal.

Table 3. *Bile samples containing mixed conjugates of glucuronide glucose and xylose.*

Notes: A, pony with intact enterohepatic circulation, T-tube opened immediately before collection; B, same conditions as A, but different pony. C, T-tube opened to external drainage for 4h (same pony as in B); D, this sample diluted 1:100, hence the lack of precision in concentration; E, F, these two samples have a UCB concentration an order of magnitude higher than any other sample assayed in the present study; a delay in placing these two samples in EDTA and ascorbic acid at -20°C may have resulted in hydrolysis of bilirubin conjugates to UCB.

Animal	Site	Notes	Peak no. on chromatogram*	[Bilirubin] (µM)										Total		
				1	2	3	4	5	6	7	8	9	10			
Pony	Hepatic	A	BDG	60.4 (2.2)	60.4 (22.4)	147.2 (54.5)	n.d.§	n.d.	n.d.	4.2 (1.6)	n.d.	n.d.	36.0 (13.3)	8.0 (3.0)	8.2 (3.0)	270.0
		B	BDG	n.d.	9.1 (11.1)	57.0 (69.8)	n.d.	n.d.	n.d.	n.d.	n.d.	n.d.	7.6 (9.3)	8.0 (9.8)	n.d.	81.7
		C	BDG	3.4 (1.2)	63.0 (21.5)	170.6 (58.2)	n.d.	n.d.	n.d.	11.6 (4.0)	n.d.	n.d.	n.d.	22.9 (7.8)	18.7 (6.4)	3.0 (1.0)
Cat	G.B.	D	BDG	6870.0 (38.6)	6660.0 (37.5)	770.0 (4.3)	n.d.	n.d.	n.d.	2640.0 (14.9)	n.d.	n.d.	650.0 (3.7)	100.0 (0.6)	n.d.	17770.0
Dog	G.B.	E	BDG	1135.9 (30.2)	1484.8 (34.5)	236.7 (6.3)	tr.	305.4 (8.1)	359.0 (9.6)	tr.	tr.	tr.	79.2 (2.1)	141.4 (3.8)	17.0 (0.5)	3759.4
Monkey	G.B.	F	BDG	3772.6 (44.8)	2185.5 (25.9)	199.7 (2.4)	tr.	234.9 (2.8)	1471.0 (17.5)	tr.	tr.	tr.	266.0 (3.1)	177.8 (2.1)	113.7 (1.4)	8421.2

\* See key in Table 1; numbers are based on the h.p.l.c. elution sequence for dog bile (Fig. 8).

† N.I., not identified.

‡ Values in parentheses are percentage concentrations; values above parentheses are concentration in µM.

§ n.d., not detected.

|| tr., trace.



Table 4. Human bile samples

Notes: A, bile from patient with previous common duct obstruction from tumour; B, ERCP bile from patient with Gilbert's syndrome and previous cholecystectomy for pigment stone 3 years before; C, ERCP bile from patient with normal biliary tree.

Animal	Site	Peak number on chromatogram* Gallstones Notes	[Bilirubin] ( $\mu\text{M}$ )									
			1 BDG	2 BMG-GI	3 BDGI	5 BMGI-MX	6 BMG	8 BMGI	9 BMX	10 UCB	Total	
Human	T-tube	—	240.6† (69.3)	45.8 (13.2)	28.6 (8.2)	1.8 (0.5)	26.5 (7.6)	n.d.	9.2 (1.2)	tr	352.5	
	T-tube	Pigment	n.d.	153.3 (60.3)	37.2 (14.6)	34.0 (13.4)	27.9 (11.0)	n.d.	1.8 (0.7)	tr	254.2	
	T-tube	—	1255.0 (87.0)	n.d.	5.6 (0.3)	n.d.	172.0 (11.9)	7.2 (0.5)	n.d.	2.0 (0.1)	1441.8	
	G.B.†	Cholesterol	2609.6 (63.8)	448.8 (11.0)	146.5 (3.6)	75.9 (1.9)	575.4 (14.1)	107.2 (2.6)	114.1 (2.8)	11.3 (0.3)	4088.8	
	ERCP	—	247.0 (50.2)	18.5 (3.8)	59.1 (12.0)	n.d.	150.5 (30.5)	3.6 (0.7)	9.4 (1.9)	3.0 (0.6)	491.6	
	ERCP	—	205.6 (50.6)	47.7 (11.8)	20.2 (5.0)	n.d.	113.8 (28.0)	5.7 (1.4)	10.1 (2.5)	2.8 (0.7)	405.9	

\* See key in Table 1; number sequence as for dog bile (Fig. 8). Peaks 4 and 7 were not detected in any human bile sample.

† Values in parentheses are percentage concentrations; values above parentheses are concentrations in  $\mu\text{M}$ .

‡ G.B., gall bladder; n.d., not determined; tr, trace.

tation of proteins, and the procedure for separation and quantification of each bile pigment is complete within approx. 25 min. With our method we have further been able to identify xylose, glucose and mixed conjugates in cat, dog, pony and human biles, and traces in certain rodent biles, indicating that this method can distinguish between individual sugar conjugates, many of which are present in small amounts. For quantification of the latter species, we assumed that the molar absorptivities of the glucose and xylose conjugates are similar to those of the glucuronide conjugates.

The method of quantification of BMG and BDG is novel because it relates concentrations of BMG and BDG to a stable azo derivative of UCB that has been crystallized for the first time in the present work. Since the glucuronide conjugates are the major pigments in man and most laboratory mammals (Fevry *et al.*, 1977), we utilized the present technique to specifically quantify and isolate pure BMG and BDG from pigment-enriched rat or guinea-pig biles. However, the glucose, xylose and mixed conjugates could also be *directly* quantified by a modification of our technique by first isolating pure BMG1 and BMX from dog bile by preparative h.p.l.c. Similar to what we have accomplished here for BMG, diazotization of the monoglucoside or the monoxyloside conjugates yields AZO·UCB, which is the basic reference standard for h.p.l.c. quantification of all mono- and di-conjugates.

Excellent correlations were found between the h.p.l.c. IPA values of bilirubin conjugates and the IPA values of their respective ethyl anthranilate diazo derivatives. The breakpoint in the standard curve of BMG at 100  $\mu$ M concentration (Fig. 5) may be the result of the self-association of BMG in aqueous-methanol systems at higher concentrations. In this regard, Carey & Koretsky (1979) deduced that dimers and higher aggregates of UCB formed at pH 10 in both aqueous and mixed aqueous-ethanol solutions. This was inferred from a concentration-dependent bathochromic shift in the absorption spectrum of UCB; we have identified a similar concentration-dependent spectral shift with BMG in aqueous and aqueous-methanol solvents (W. Spivak & M. C. Carey, unpublished work).

The most popular previously used procedure for quantification of bilirubin conjugates has utilized the ethyl anthranilate diazo method (Heirwegh *et al.*, 1974); however, this method gives only percentage concentrations of the glucuronide, glucose, xylose and unconjugated azodipyrroles and an estimate of the total monoconjugated fraction. Since the diazo reaction cleaves bilirubin into two azodipyrrolic units, the method cannot reveal the original tetrapyrrolic structure, particularly in the

case of mixed bilirubin conjugates. Nonetheless, our method gives comparable results (data is available from W.S. or M.C.C.) to the diazo method (Fevry *et al.*, 1977) for the percentage of monoconjugates and the proportion of conjugated azodipyrroles in most bile samples.

Because of the clinical relevance of animal models of gallstone formation, we have applied our method to the analysis of bile samples from the spherocytic deer mouse, a model for human hereditary spherocytosis (Anderson *et al.*, 1966; Bernstein, 1980). As a result of chronic haemolysis, this species excretes a greater concentration of bilirubin conjugates, as shown in Fig. 7 and Table 2. The gall-bladder bile of the spherocytic deer mouse contains more than four times as much BMG and a 3-fold (average of two animals) increase in UCB concentration compared with that in the normal deer mouse. It is presumed that the poor solubility of UCB in bile (Berman *et al.*, 1980; Soloway *et al.*, 1977) at neutral pH results in calcium-salt precipitation and pigment stone formation.

We have also demonstrated here that the normal deer mouse, guinea pig, hamster and prairie dog, all models for both pigment (Okey, 1944; Anderson *et al.*, 1966; DiFilippo & Blumenthal, 1972; Pitt *et al.*, 1983) and cholesterol gallstones (Van der Linden & Bergman, 1979), excrete BMG almost exclusively (Fig. 7, Table 2). In view of the instability of the BMG molecule and its presence as the only conjugate in four animal models of pigment-gallstone formation, it seems plausible that it may play a central role in the formation of gallstones. One possible explanation is that UCB found in bile is not just a result of increased concentration of secreted UCB, but is a direct result of BMG degradation, either enzymically (via hydrolysis from biliary ductular  $\beta$ -glucuronidase) or non-enzymically by spontaneous hydrolysis of the glucuronide sugars or by molecular rearrangement, as shown here (Fig. 4).

Although BMG solubility has never been studied directly, the h.p.l.c. elution pattern supports the hypothesis that BMG has a much lower aqueous solubility than BDG. The h.p.l.c. retention time on a reverse-phase column is a direct function of the hydrophilic-hydrophobic balance of a compound, and hence reflects the aqueous solubility of a biological amphiphile (Armstrong & Carey, 1982). Thus one expects that the diconjugates of bilirubin should be more water-soluble than the monoconjugates (e.g., BDG > BMG), and that the glucuronic acid conjugates should be more soluble than the glucose or xylose conjugates. In model bile systems, BMG can co-precipitate with UCB (W. Spivak and M.C. Carey, unpublished work). However, the physical-chemical factors

that influence the solubility of BMG or BDG and the isomerization or hydrolysis of BMG to UCB in bile have yet to be clearly defined.

We believe that bile-pigment quantification by the h.p.l.c. method described in the present work is the most facile and accurate to date, particularly in view of the lability of these compounds, especially when separated on silica gel by t.l.c. A t.l.c. method (Boonyapisit *et al.*, 1976) has been employed by several investigators (Boonyapisit *et al.*, 1978; Masuda & Nakayama, 1979; Trotman *et al.*, 1980; Tritapepe *et al.*, 1980) to determine the concentration of UCB in control and pigment-stone gallbladder biles of both humans and normoblastic (*nb/nb*) mice. The reported mean values for [UCB] range from 14 to 33  $\mu\text{M}$  in control biles and 26 to 181  $\mu\text{M}$  in pigment-lithogenic biles. In contrast, by the h.p.l.c. method described here, the mean UCB concentrations found in fresh mammalian biles with pigment gallstones were 13  $\mu\text{M}$  and, in those without pigment gallstones, were 5  $\mu\text{M}$ . We believe that the use of the t.l.c. method (Boonyapisit *et al.*, 1976) may give falsely elevated [UCB] values, as a result of spontaneous hydrolysis of bilirubin conjugates on the stationary silica phase. Finally, the h.p.l.c. preparative isolation of pure BMG and BDG from bile in high concentrations will undoubtedly be important for future physical-chemical research with these compounds.

This work was supported in part by NIADDK (National Institute of Arthritis, Diabetes, Digestive and Kidney Diseases) Research Grant AM 18559 and a grant from the Cystic Fibrosis Foundation (to M.C.C.). W.S. was supported by NIADDK Training Grant AM 07333 and a grant-in-aid from the American Liver Foundation. We are grateful to Ms. Rebecca Ankener for her secretarial and editorial assistance, and to Dr. Richard Grand for his encouragement and support.

## References

- Admirand, W. H. & Small, D. M. (1968) *J. Clin. Invest.* **47**, 1043–1052
- Anderson, R., Huestis, R. R. & Motulsky, A. G. (1966) *Blood* **15**, 491–503
- Armstrong, M. J. & Carey, M. C. (1982) *J. Lipid Res.* **23**, 70–80
- Bartlett, G. R. (1959) *J. Biol. Chem.* **234**, 466–468
- Berman, M. D., Koretsky, A. P. & Carey, M. C. (1980) *Gastroenterology*, **78**, 1141 (abstr.)
- Bernstein, S. E. (1980) *Lab. Animal. Sci.* **30**, 197–205
- Blanckaert, N. (1980) *Biochem. J.* **185**, 115–128
- Blanckaert, N. & Schmid, R. (1982) in *Hepatology – A Textbook of Liver Disease* (Zakim, D. & Boyer, T. D., eds.), pp. 246–296, W.B. Saunders, Philadelphia
- Blanckaert, N., Kabra, P. M., Farina, F. A., Stafford, B. E., Marton, L. J. & Schmid, R. (1980) *J. Lab. Clin. Med.* **96**, 198–212
- Boonyapisit, S. T., Trotman, B. W., Ostrow, J. D., Olivieri, P. J. & Gallo, D. (1976) *J. Lab. Clin. Med.* **85**, 857–863
- Boonyapisit, S. T., Trotman, B. W. & Ostrow, J. D. (1978) *Gastroenterology* **74**, 70–74
- Brodersen, R. (1979) *J. Biol. Chem.* **254**, 2364–2369
- Carey, M. C. & Koretsky, A. P. (1979) *Biochem. J.* **179**, 675–689
- Chowdhury, J. R., Chowdhury, N. R., Wu, G., Shouval, R. & Arias, I. M. (1981) *Hepatology* **1**, 622–627
- Chowdhury, N. R., Gartner, U., Wokoff, W. A. & Arias, I. M. (1982) *J. Clin. Invest.* **69**, 595–603
- Compennolle, F., Hansen, F. H. & Heirwegh, K. P. M. (1970) *Biochem. J.* **120**, 891–894
- Compennolle, F., Toppet, S. & Hutchinson, D. W. (1980) *Tetrahedron* **36**, 2237–2240
- DiFilippo, N. M. & Blumenthal, H. J. (1972) *J. Am. Osteopath. Assoc.* **72**, 288–293
- Fevry, J., Van Damme, B., Michiels, R., De Groote, J. & Heirwegh, K. P. M. (1972) *J. Clin. Invest.* **51**, 2482–2492
- Fevry, J., Van de Vijver, M., Michiels, R. & Heirwegh, K. P. M. (1977) *Biochem. J.* **164**, 737–746
- Fromm, H., Amin, P., Klein, H. & Kupke, I. (1980) *J. Lipid Res.* **21**, 259–261
- Gordon, E. R., Chan, T.-H., Samodai, K. & Goresky, C. A. (1977) *Biochem. J.* **167**, 1–8
- Garantz, D., Laker, M. F. & Hofmann, A. F. (1981) *J. Lipid Res.* **22**, 373–376
- Heirwegh, K. P. M., Fevry, J., Meuwissen, J. A. T. P., De Groote, J., Compennolle, F., Desmet, V. & Van Roy, F. P. (1974) *Methods Biochem. Anal.* **22**, 205–250
- Jansen, P. L. M. (1973) *Clin. Chim. Acta* **49**, 233–240
- Kuenzle, C. C., Sommerhalder, M., Rüttner, J. R. & Maier, C. (1966a) *J. Lab. Clin. Med.* **67**, 282–293
- Kuenzle, C. C., Maier, C. & Rüttner, J. R. (1966b) *J. Lab. Clin. Med.* **67**, 294–306
- Masuda, H. & Nakayama, F. (1979) *J. Lab. Clin. Med.* **93**, 353–366
- McDonagh, A. F. & Assisi, F. (1971) *FEBS Lett.* **18**, 315–317
- McDonagh, A. F. & Assisi, F. (1972) *Biochem. J.* **129**, 797–800
- Okey, R. (1944) *J. Biol. Chem.* **156**, 179–190
- Onishi, S., Itoh, S., Kawade, N., Isobe, K. & Sugiyama, S. (1980) *Biochem. J.* **185**, 281–284
- Pitt, H. A., Doty, J. E., Lewinski, M. A., Porter-Fink, V. & DenBesten, L. (1983) *Clin. Res.* **31**, 243A (abstr.)
- Sieg, A., Gustaff, P., Van Hees, P. & Heirwegh, K. P. M. (1982) *J. Clin. Invest.* **69**, 347–357
- Soloway, R. D., Trotman, B. W. & Ostrow, J. D. (1977) *Gastroenterology* **72**, 167–182
- Talalay, P. (1960) *Methods Biochem. Anal.* **8**, 119–143
- Tritapepe, R., Padova, C. D. & Rovagnati, P. (1980) *Br. Med. J.* **280**, 832
- Trotman, B. W., Bernstein, S. E., Bove, K. E. & Wirt, G. D. (1980) *J. Clin. Invest.* **65**, 1301–1308
- Van der Linden, W. & Bergman, F. (1979) *Int. Rev. Exp. Pathol.* **17**, 173–233
- Van Roy, R. P. & Heirwegh, K. P. M. (1968) *Biochem. J.* **107**, 507–518
- Weiss, J. S., Gautam, A., Lauff, J. J., Sundberg, M. W., Jatlow, P., Boyer, J. L. & Seligson, D. (1983) *N. Engl. J. Med.* **309**, 147–150
- Woolridge, T. A. & Lightner, D. A. (1978) *J. Liq. Chromatogr.* **1**, 653–658